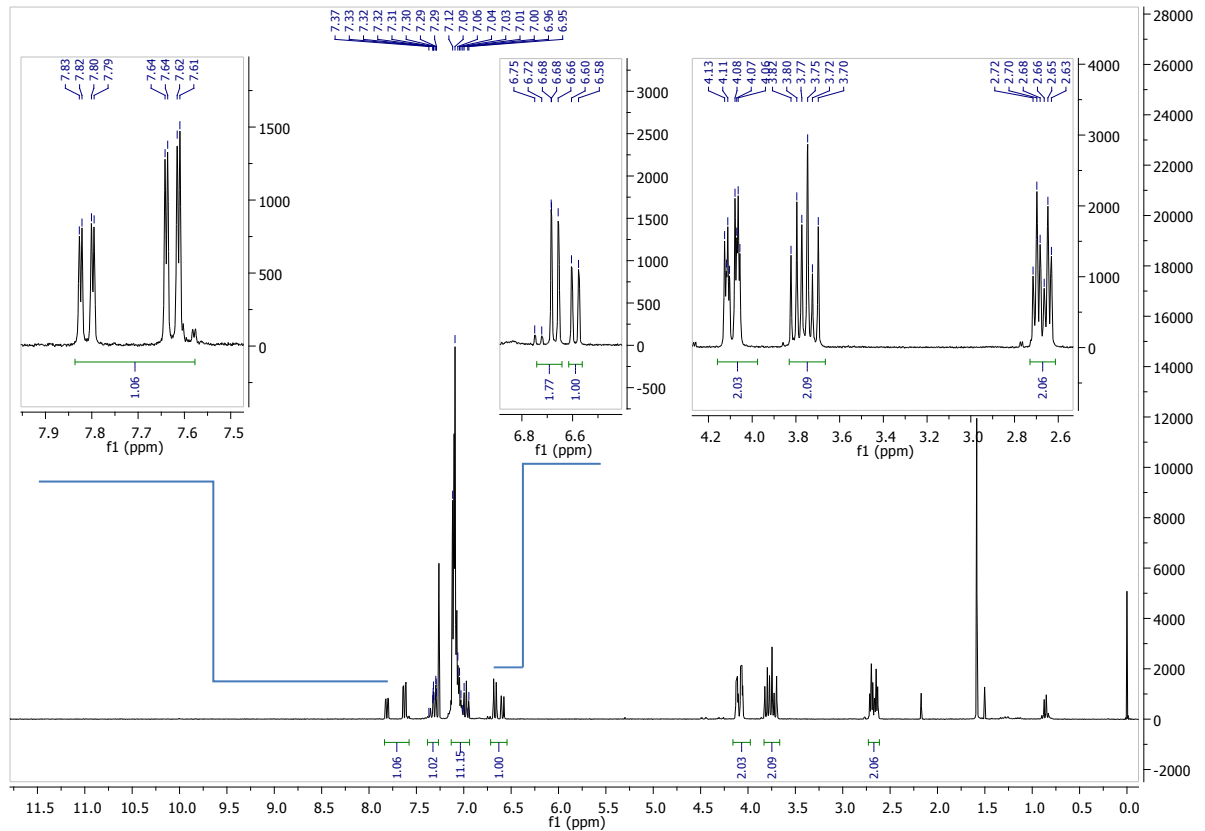


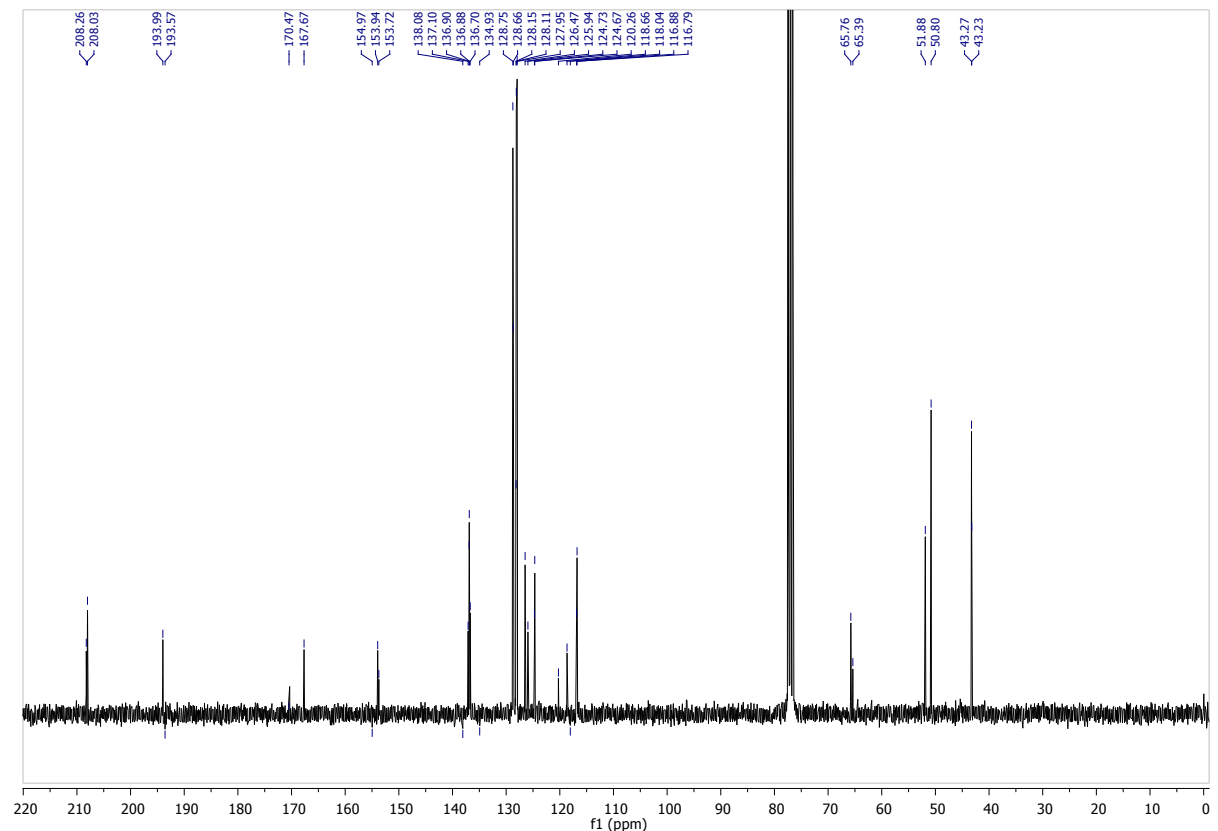
## Supplementary Material

### Table of Contents:

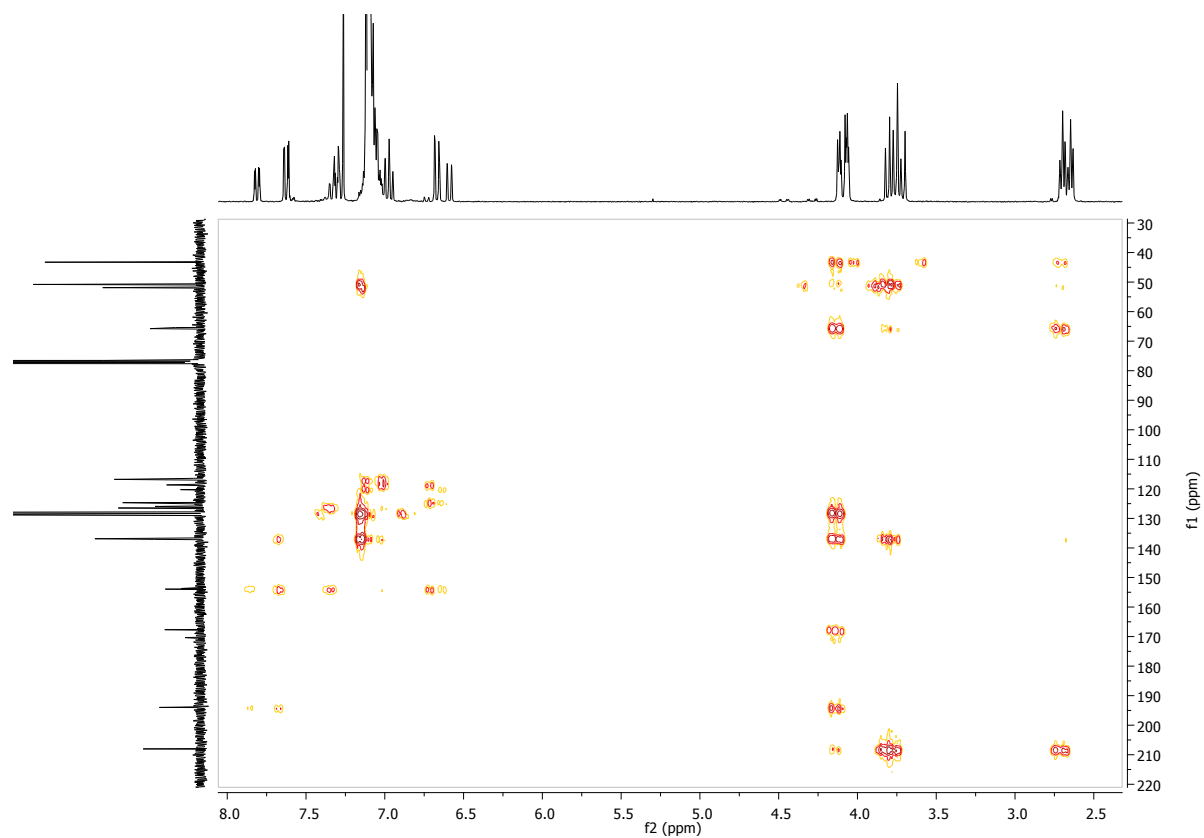
|  |    |
|--|----|
| <b>Figure 1.</b> $^1\text{H}$ NMR spectrum of compound <b>4a</b> (500.13 MHz)              | 2  |
| <b>Figure 2.</b> $^{13}\text{C}$ NMR spectrum of compound <b>4a</b> (125.77 MHz)           | 2  |
| <b>Figure 3.</b> HMBC NMR spectrum of compound <b>4a</b>                                   | 3  |
| <b>Figure 4.</b> Partial HMBC NMR spectrum of compound <b>4a</b>                           | 3  |
| <b>Figure 5.</b> $^1\text{H}$ NMR spectrum of compound <b>5</b> (500.13 MHz)               | 4  |
| <b>Figure 6.</b> $^{13}\text{C}$ NMR spectrum of compound <b>5</b> (125.77 MHz)            | 4  |
| <b>Figure 7.</b> $^1\text{H}$ NMR spectrum of compound <b>4b</b> (500.13 MHz)              | 5  |
| <b>Figure 8.</b> $^{13}\text{C}$ NMR spectrum of compound <b>4b</b> (125.77 MHz)           | 5  |
| <b>Figure 9.</b> HMBC NMR spectrum of compound <b>4b</b>                                   | 6  |
| <b>Figure 10.</b> Partial NOESY NMR spectrum of compound <b>4b</b>                         | 6  |
| <b>Figure 11.</b> $^1\text{H}$ NMR spectrum of compound <b>4c</b> (500.13 MHz)             | 7  |
| <b>Figure 12.</b> $^{13}\text{C}$ NMR spectrum of compound <b>4c</b> (125.77 MHz)          | 7  |
| <b>Figure 13.</b> HMBC NMR spectrum of compound <b>4c</b>                                  | 8  |
| <b>Figure 14.</b> Partial HMBC NMR spectrum of compound <b>4c</b>                          | 8  |
| <b>Figure 15.</b> $^1\text{H}$ NMR spectrum of compound <b>4d</b> (500.13 MHz)             | 9  |
| <b>Figure 16.</b> $^{13}\text{C}$ NMR spectrum of compound <b>4d</b> (125.77 MHz)          | 9  |
| <b>Figure 17.</b> $^1\text{H}$ NMR spectrum of compound <b>4e</b> (500.13 MHz)             | 10 |
| <b>Figure 18.</b> $^{13}\text{C}$ NMR spectrum of compound <b>4e</b> (125.77 MHz)          | 10 |
| <b>Figure 19.</b> $^1\text{H}$ NMR spectrum of compound <b>4f</b> (500.13 MHz)             | 11 |
| <b>Figure 20.</b> $^{13}\text{C}$ NMR spectrum of compound <b>4f</b> (125.77 MHz)          | 11 |
| Chiral-HPLC separation of spiro[cyclohexanone-pyrandione] exo/endo diastereomers           | 12 |
| Single-Crystal X-ray Diffraction Studies for compounds <b>4b</b> , <b>4e</b> and <b>4f</b> | 12 |
| References   | 14 |



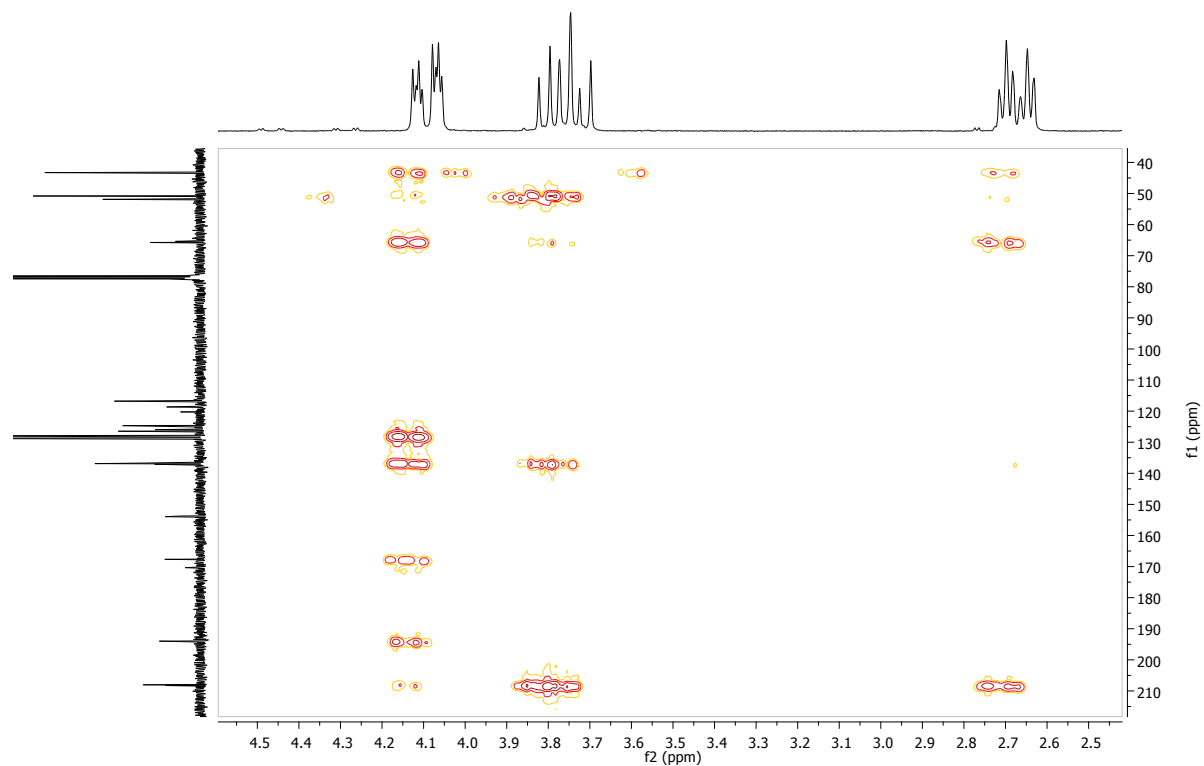
**Figure 1.**  $^1\text{H}$  NMR spectrum of compound **4a** (500.13 MHz)



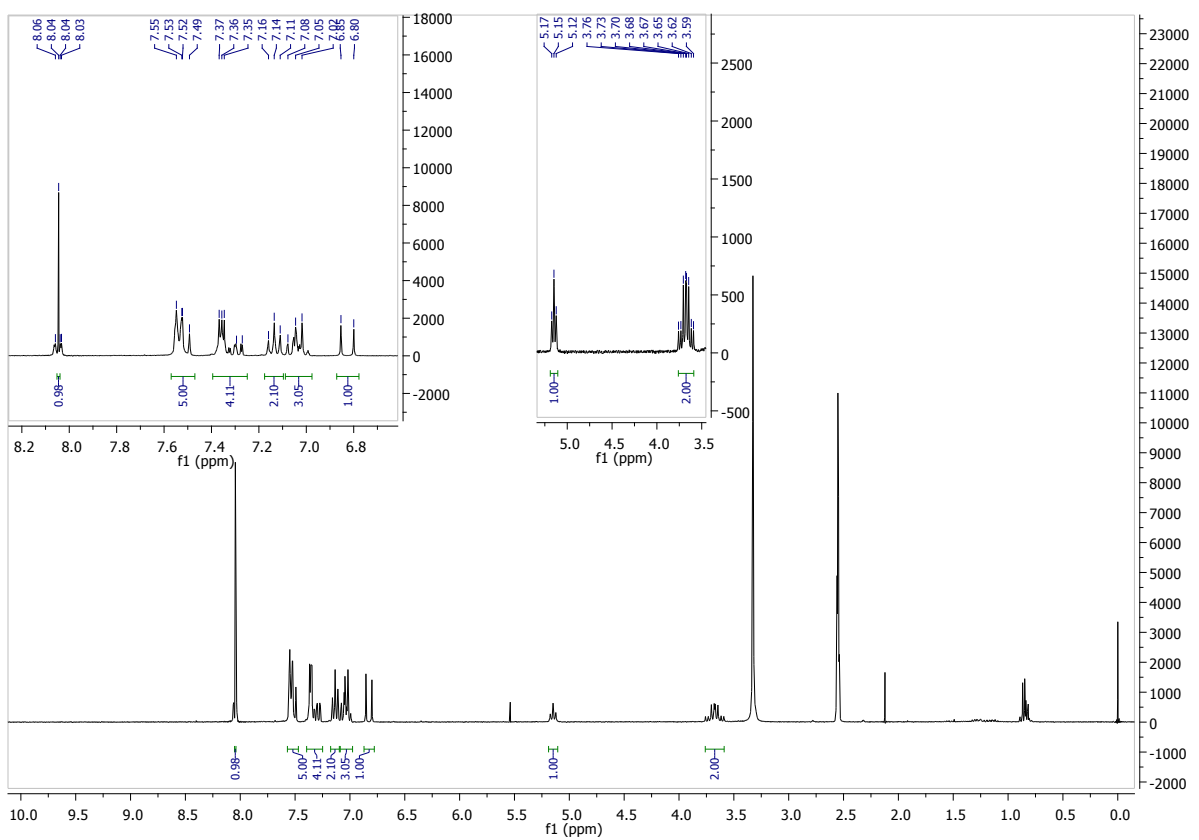
**Figure 2.**  $^{13}\text{C}$  NMR spectrum of compound **4a** (125.77 MHz)



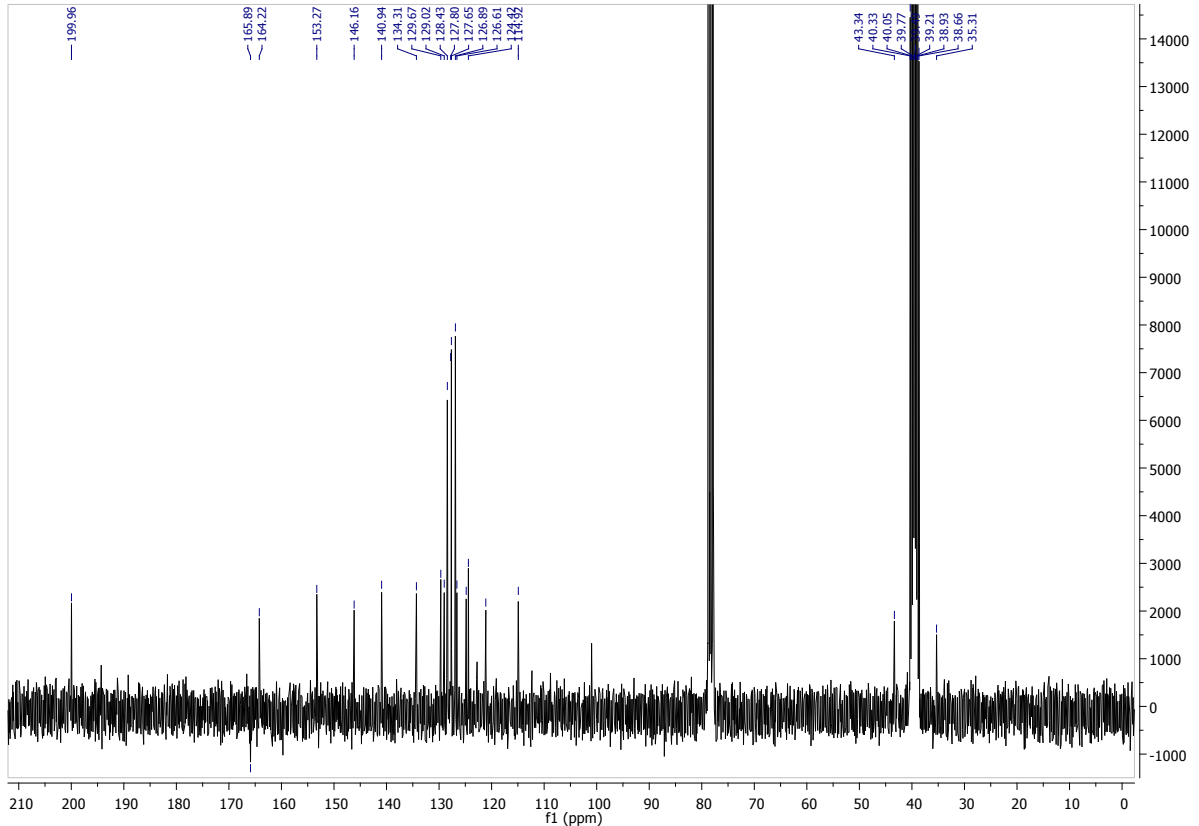
**Figure 3.** HMBC NMR spectrum of compound **4a**



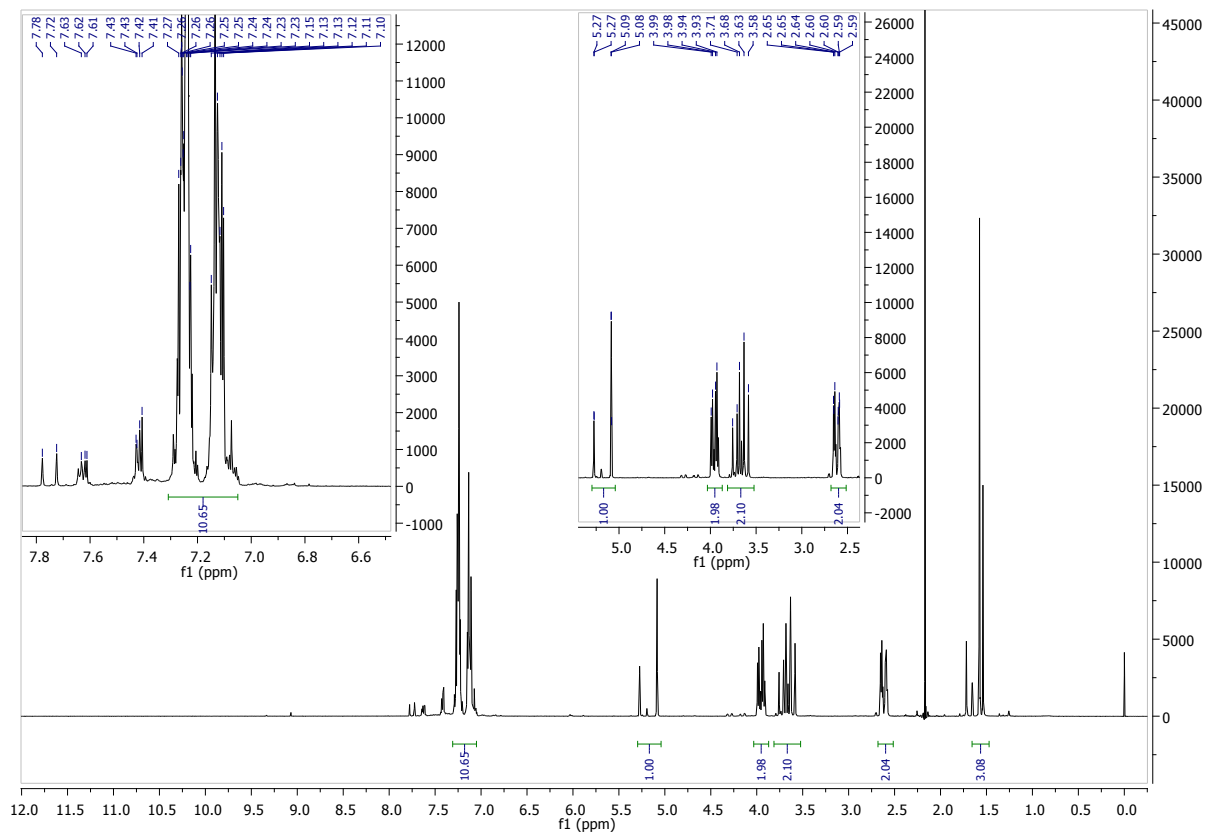
**Figure 4.** Partial HMBC NMR spectrum of compound **4a**



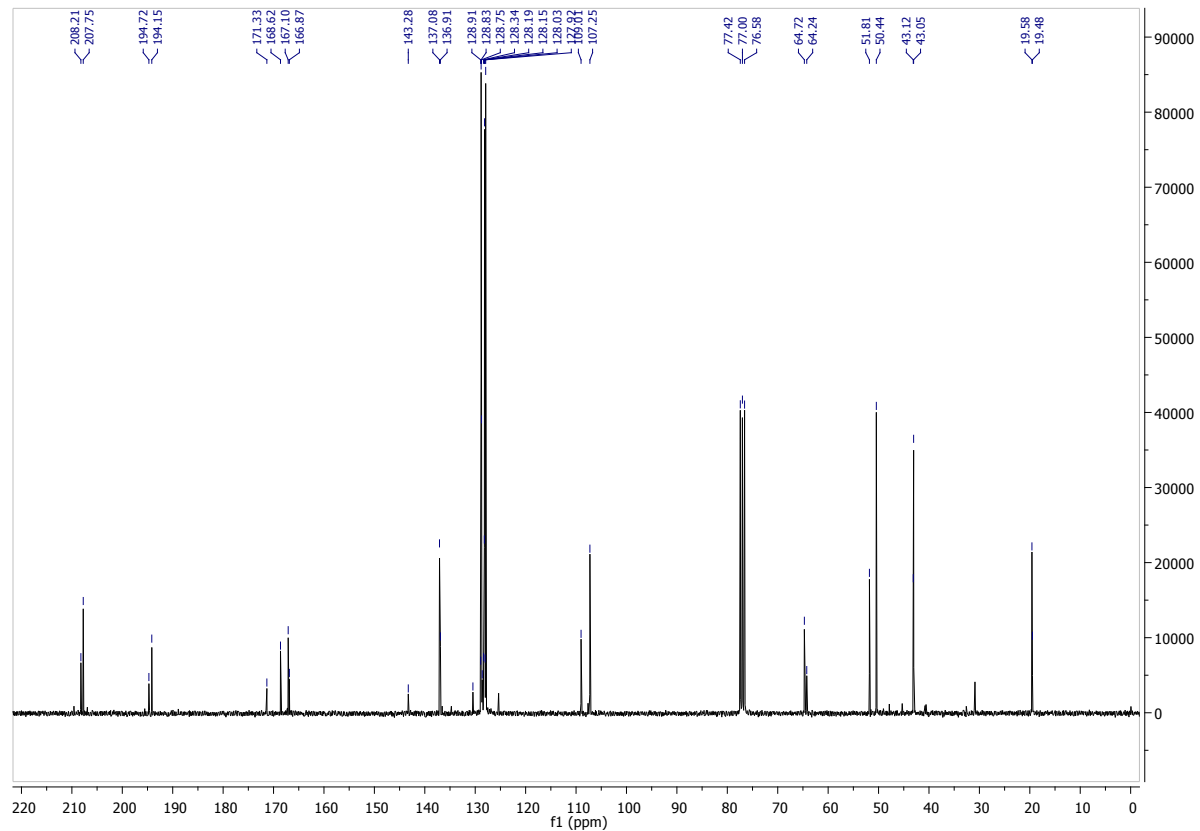
**Figure 5.**  $^1\text{H}$  NMR spectrum of compound 5 (500.13 MHz)



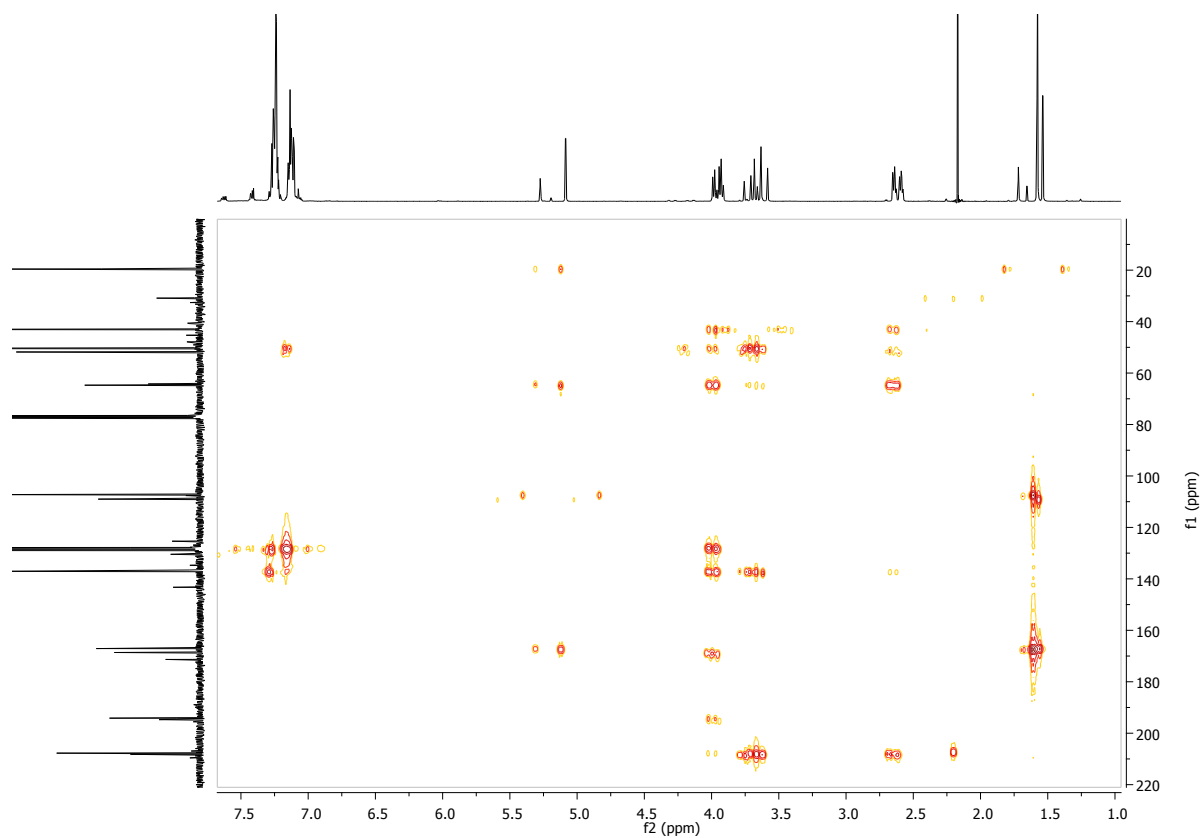
**Figure 6.**  $^{13}\text{C}$  NMR spectrum of compound 5 (125.77 MHz)



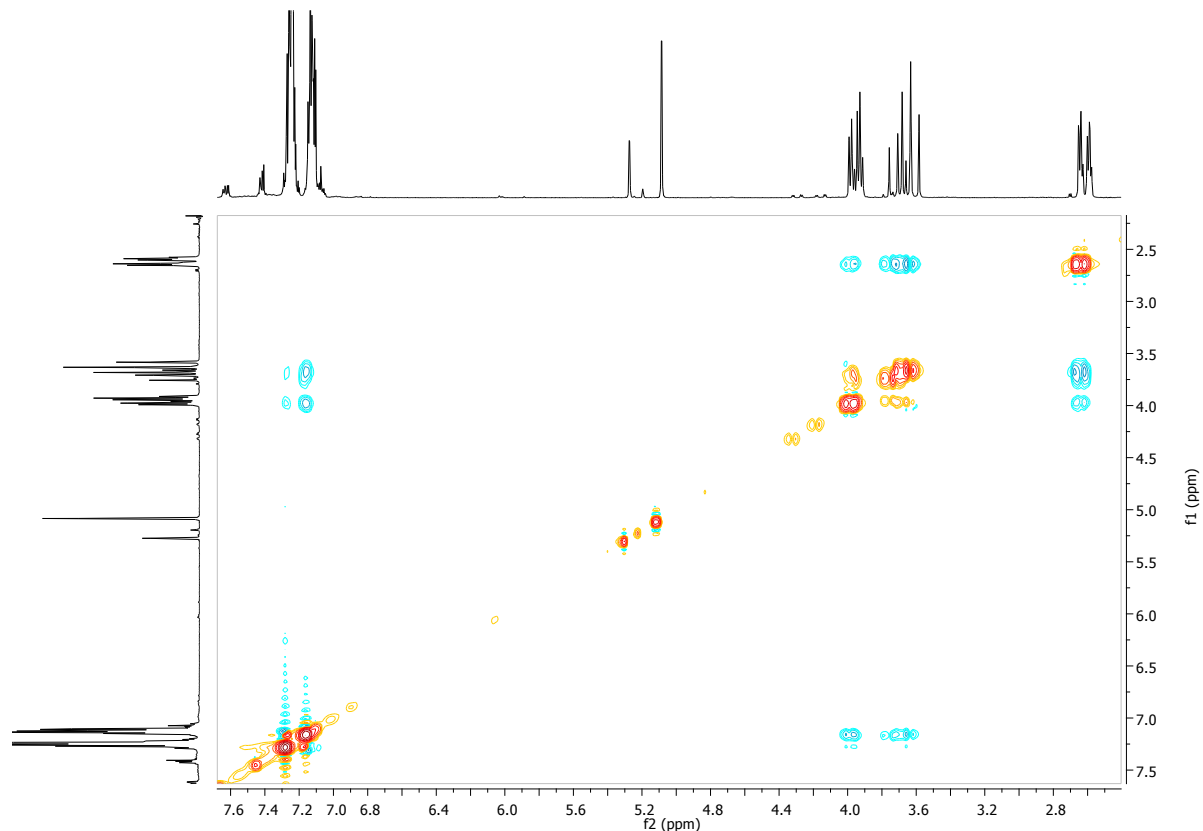
**Figure 7.**  $^1\text{H}$  NMR spectrum of compound **4b** (500.13 MHz)



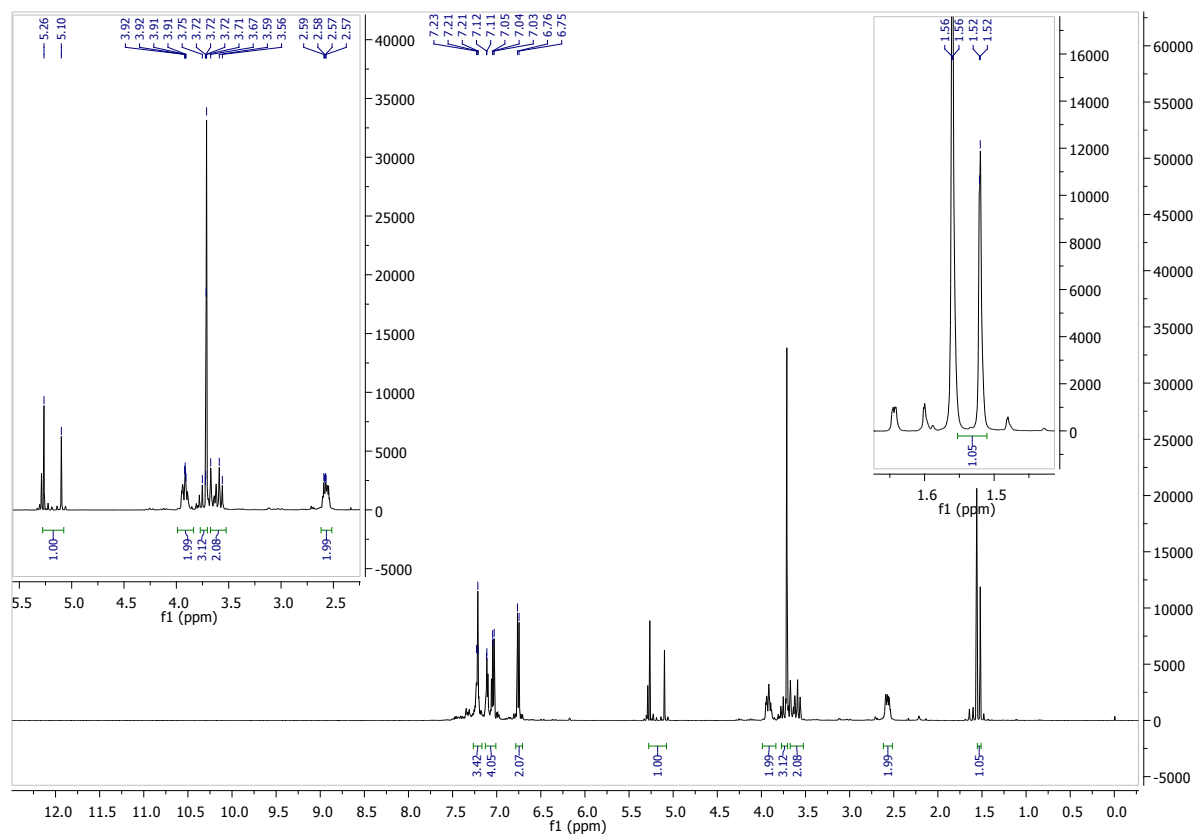
**Figure 8.**  $^{13}\text{C}$  NMR spectrum of compound **4b** (125.77 MHz)



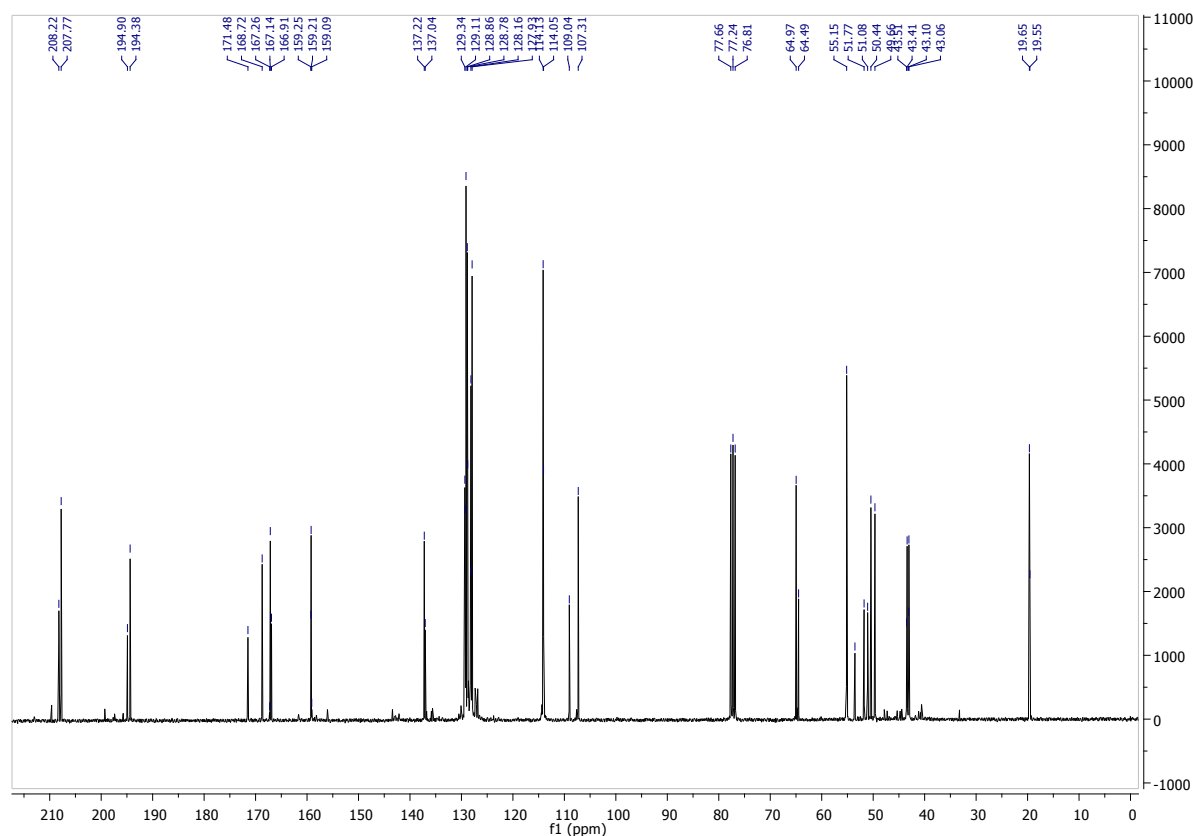
**Figure 9.** HMBC NMR spectrum of compound 4b



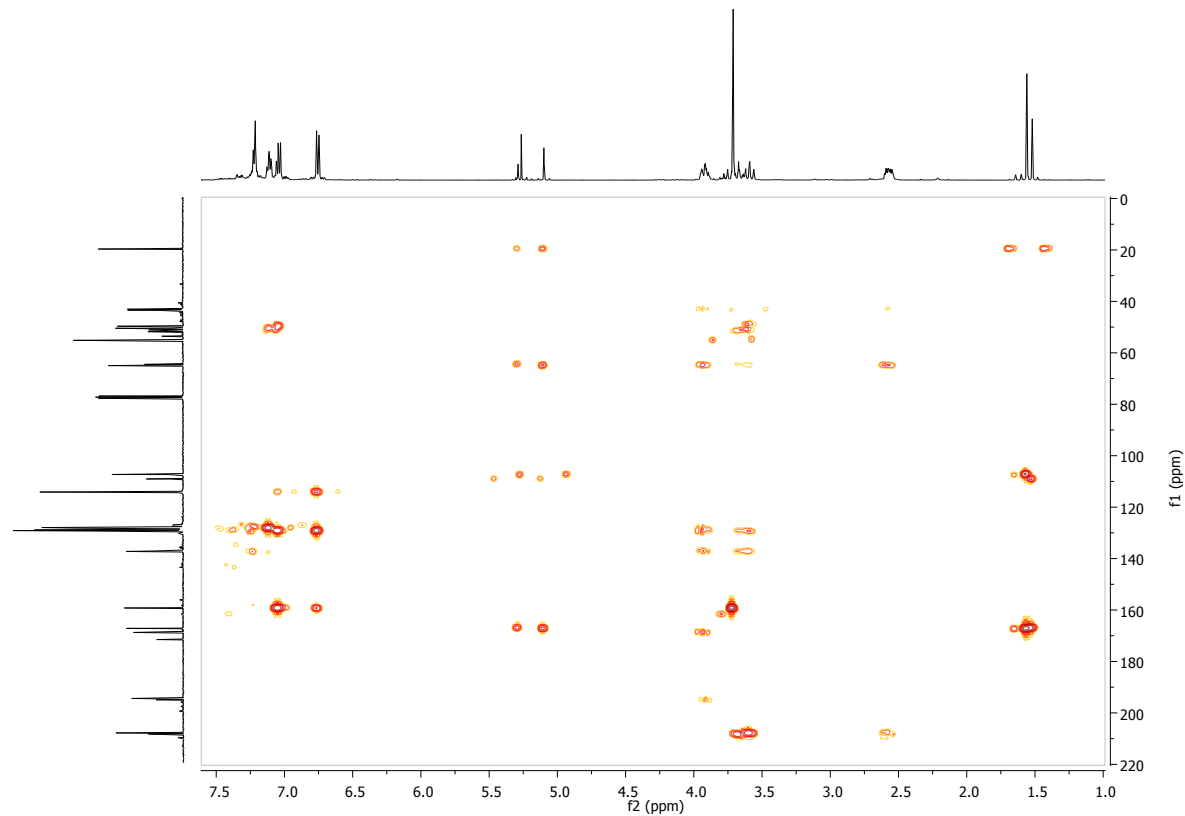
**Figure 10.** Partial NOESY NMR spectrum of compound 4b



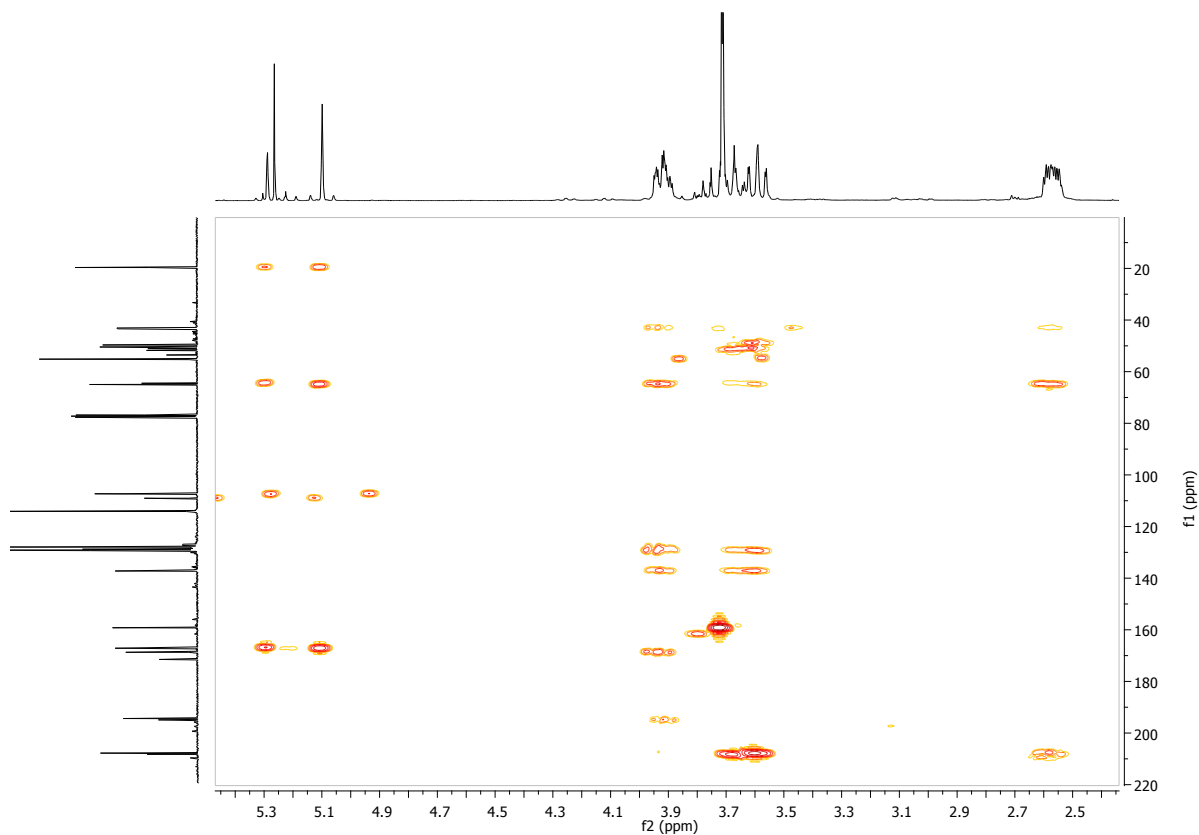
**Figure 11.** <sup>1</sup>H NMR spectrum of compound **4c** (500.13 MHz)



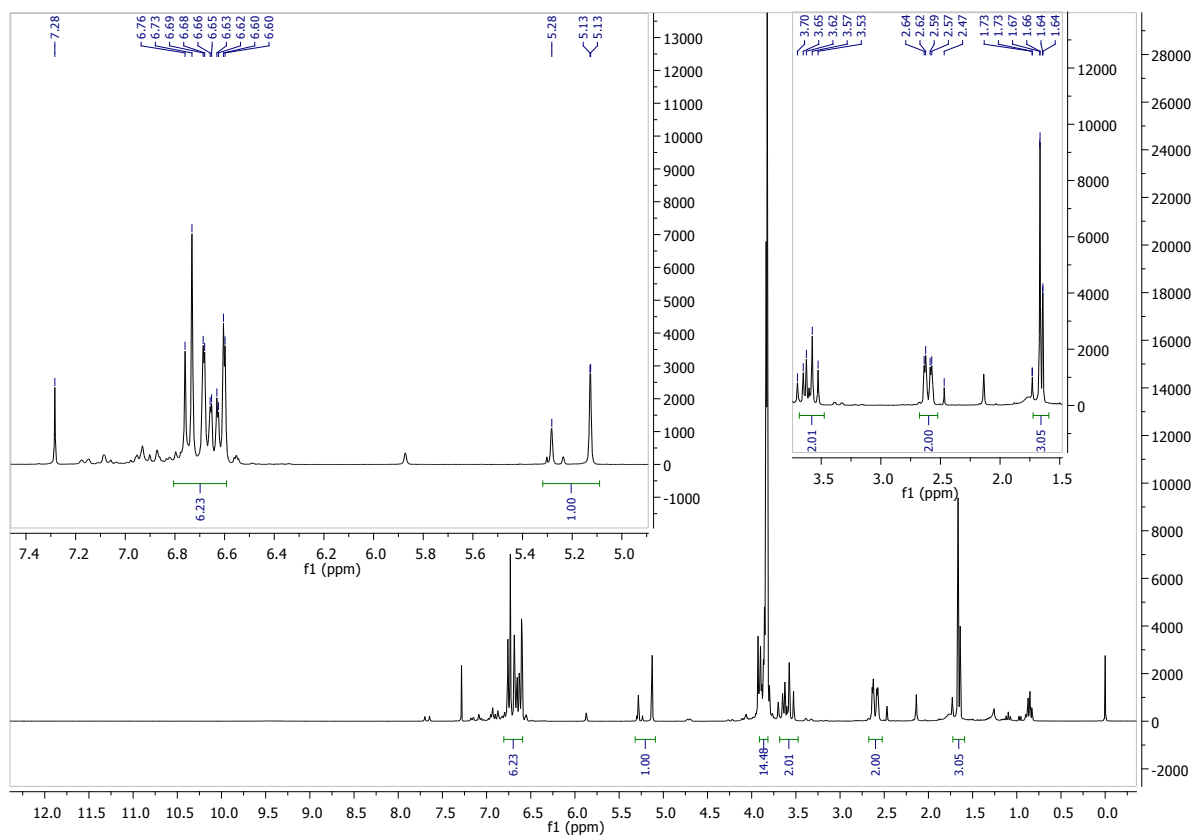
**Figure 12.** <sup>13</sup>C NMR spectrum of compound **4c** (125.77 MHz)



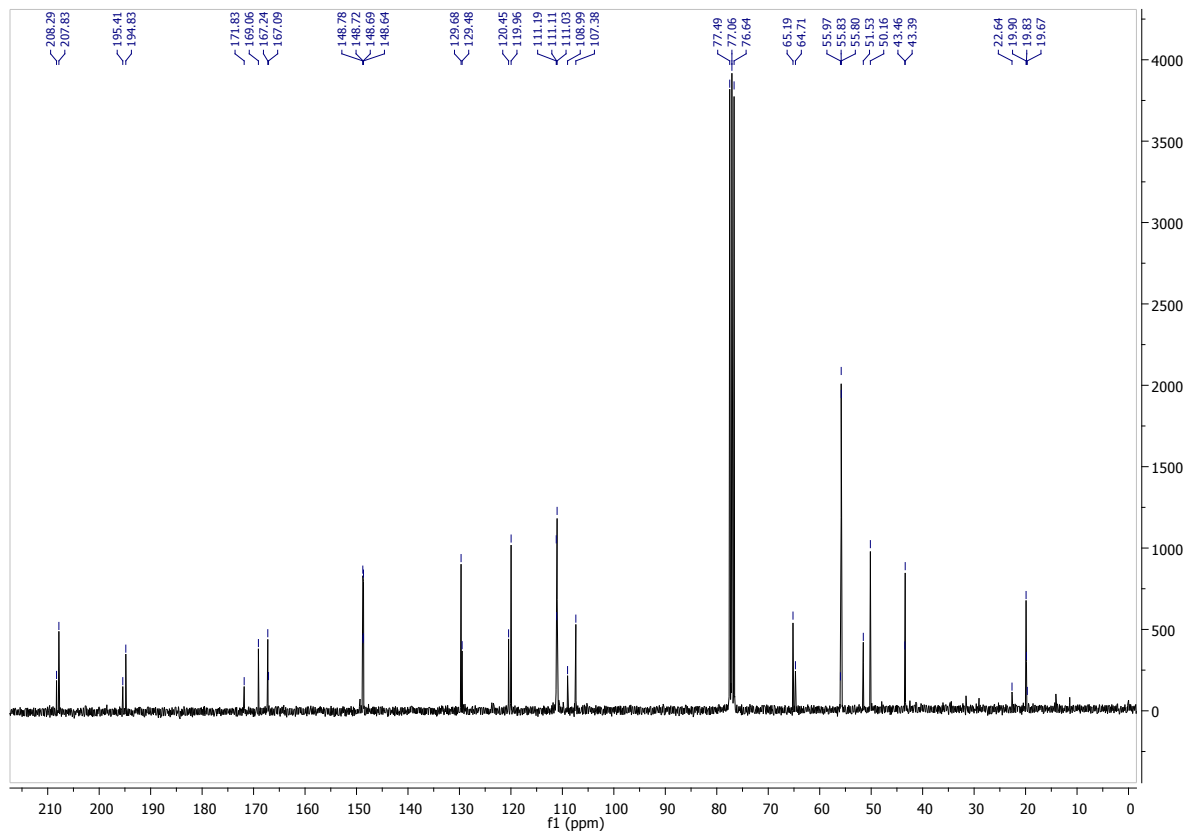
**Figure 13.** HMBC NMR spectrum of compound **4c**



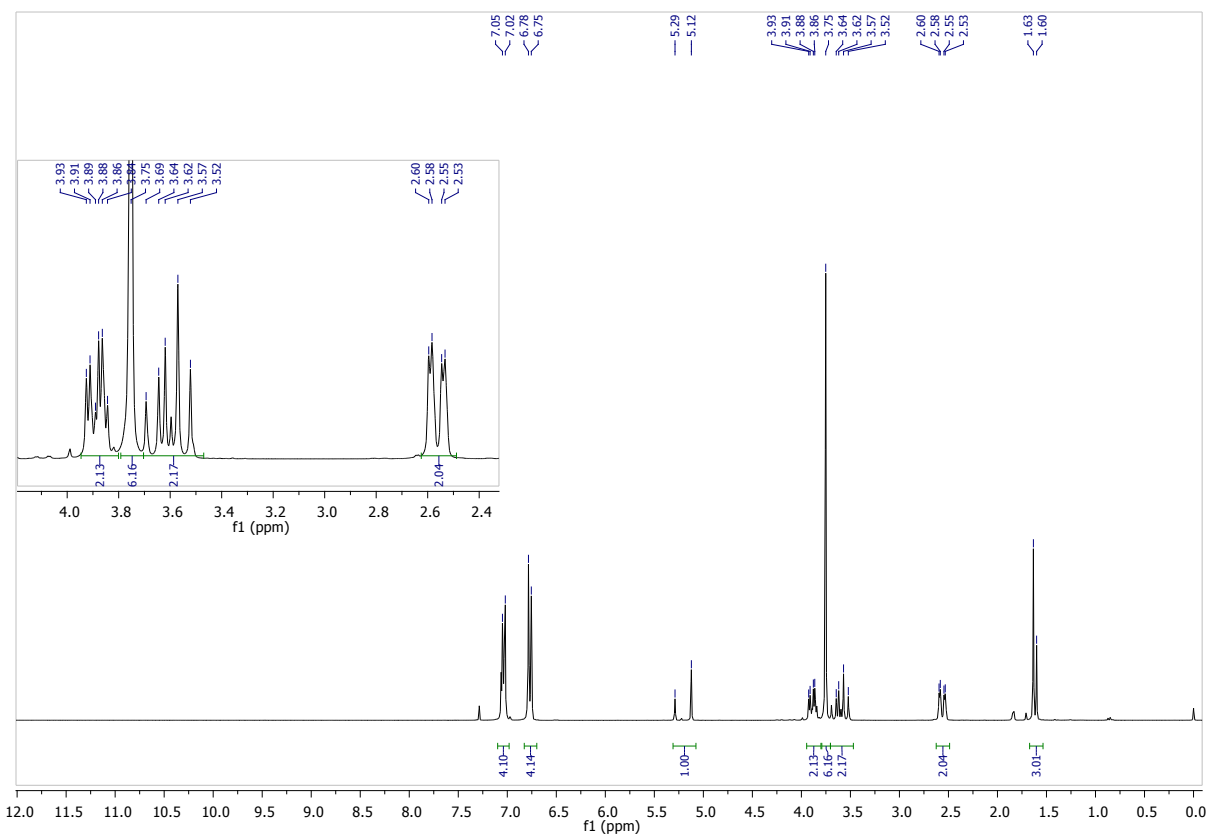
**Figure 14.** Partial HMBC NMR spectrum of compound **4c**



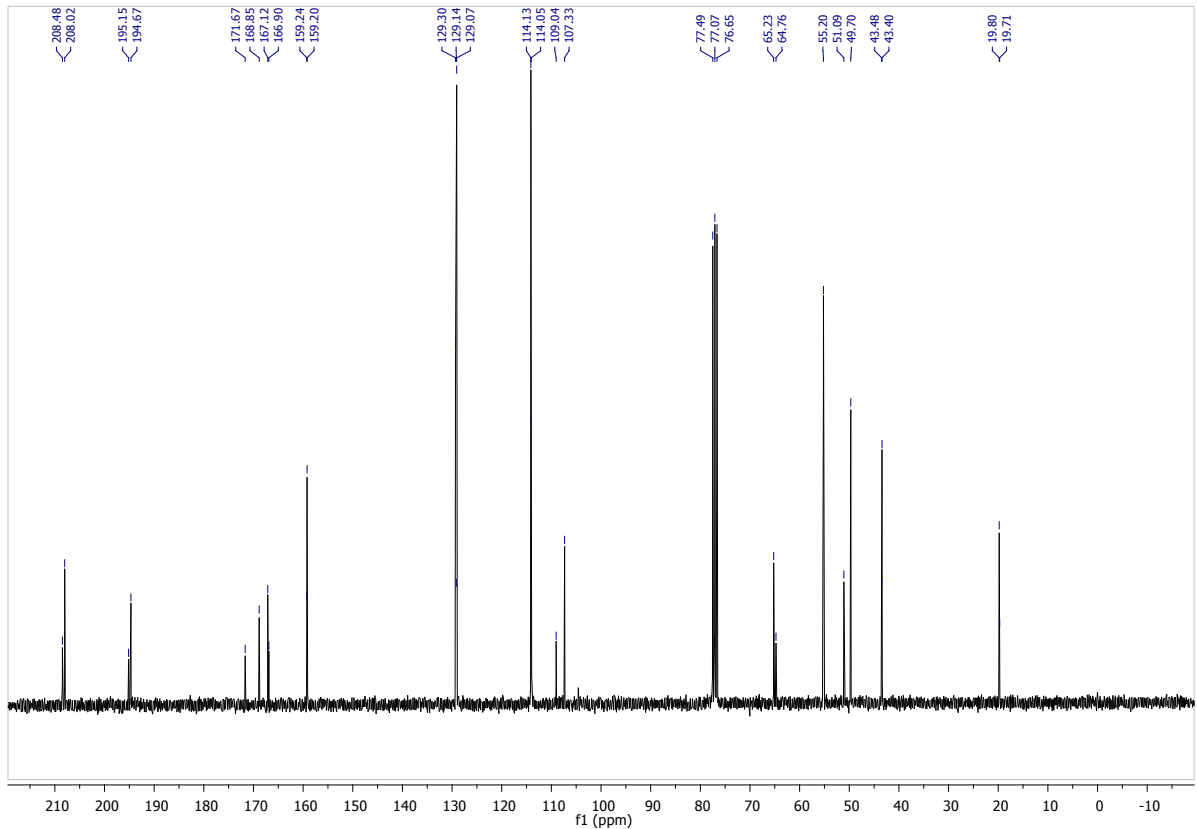
**Figure 15.**  $^1\text{H}$  NMR spectrum of compound **4d** (500.13 MHz)



**Figure 16.**  $^{13}\text{C}$  NMR spectrum of compound **4d** (125.77 MHz)



**Figure 17.**  $^1\text{H}$  NMR spectrum of compound **4e** (500.13 MHz)



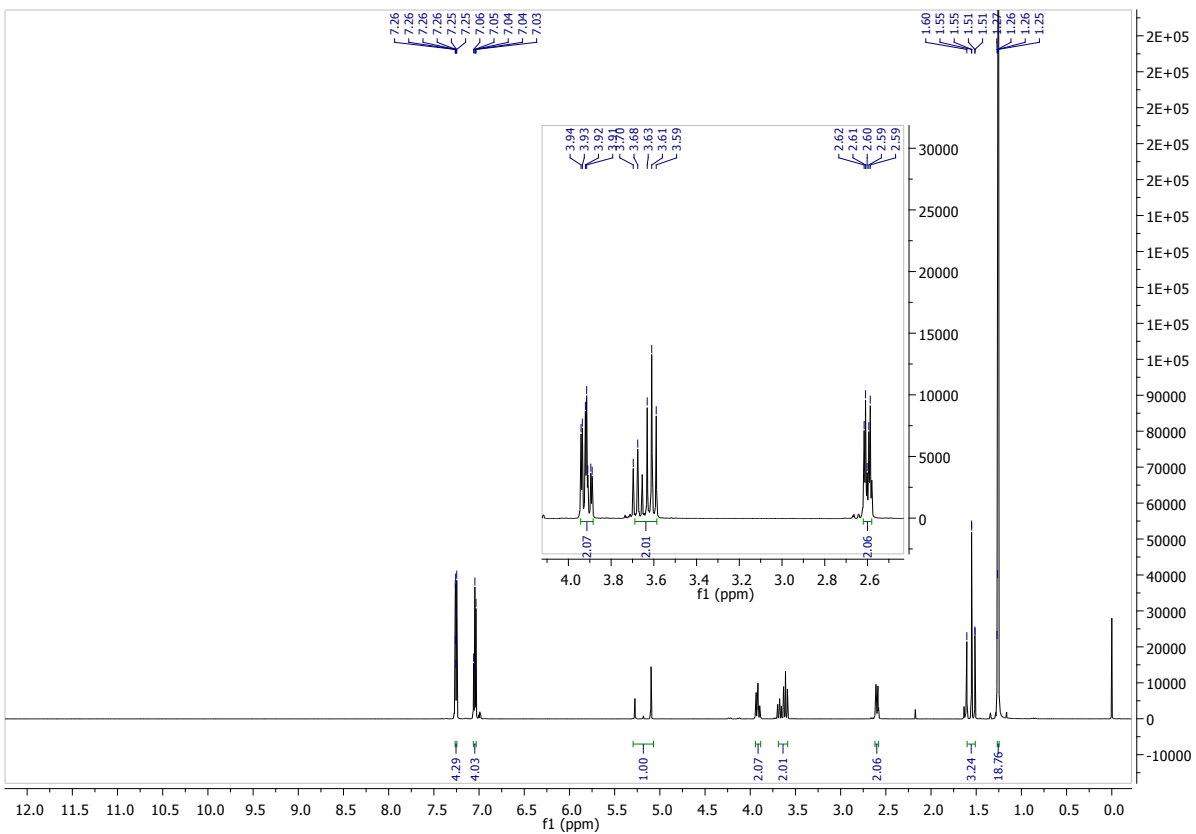


**Figure 19.**  $^1\text{H}$  NMR spectrum of compound **4f** (500.13 MHz)

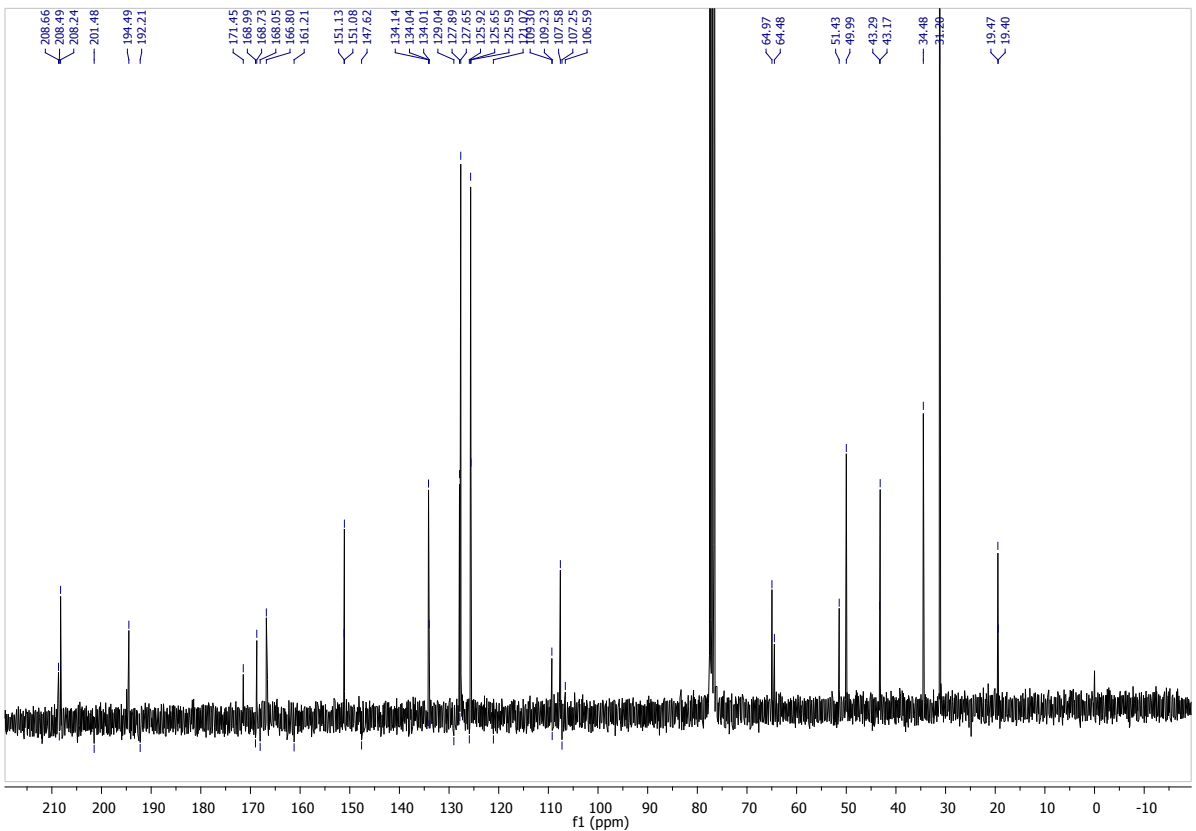


**Figure 20.**  $^{13}\text{C}$  NMR spectrum of compound **4f** (125.77 MHz)

### **Chiral-HPLC separation of spiro[cyclohexanone-pyrandione] exo/endo diastereomers**

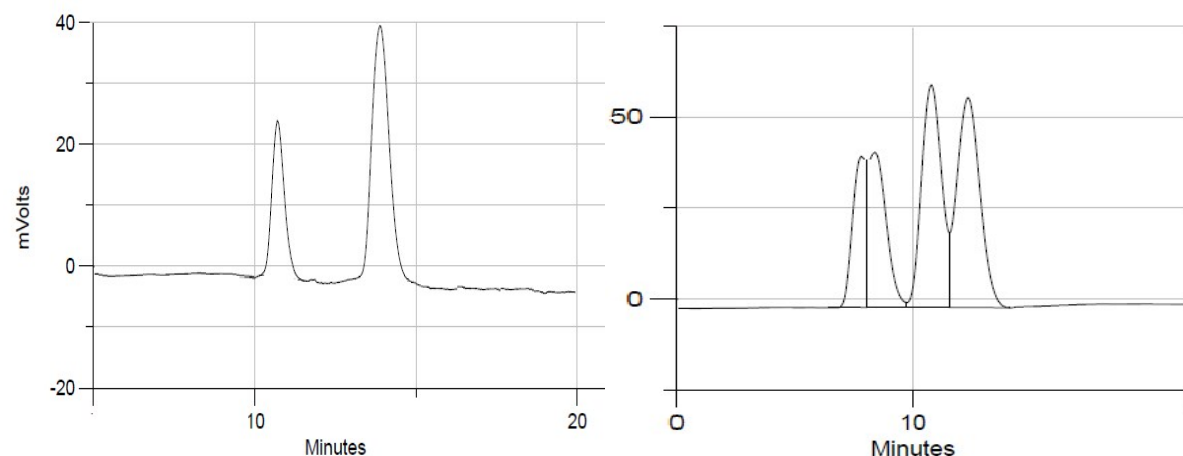


**Figure 21.** Chiral-HPLC separation of spiro[cyclohexanone-pyrandione] diastereomers of the *racemate*-compound **4c** (right) and *meso*-compound **4e** (left).

**Conditions:** Chiral-HPLC separation of the spiro[cyclohexanone-pyrandione] exo/endo diastereomers of the meso-compound **4e** and the enantiomers of the racemic-compound **4c** were performed on chiral stationary phase at 25 °C using a CHIRALCEL® OD column (particle size 10 µm, 250 x 4.6 mm ID). The mobile phase used was hexane/THF [isocratic mode, 80:20 (v/v)] at a flow rate of 1.0 mL/min. The UV detector was set at 254 nm. An injection of 20 µL of 1.0 g/L concentrated samples of compounds **4c** and **4e** in THF was used.

### **Single-Crystal X-ray Diffraction Studies for compounds **4b**, **4e** and **4f****

Single crystals of compounds **4b**, **4e** and **4f** were manually harvested from the crystallization vials and immersed in highly viscous FOMBLIN Y perfluoropolyether vacuum oil (LVAC 140/13, Sigma-Aldrich) to avoid degradation caused by the evaporation of the solvent.<sup>[1]</sup> Crystals were mounted on Hampton Research CryoLoops, typically the help of a Stemi 2000 stereomicroscope equipped with Carl Zeiss lenses.

Crystal data for **4b** were collected at 150(2)K on a Bruker X8 Kappa APEX II CCD area-detector diffractometer (Mo K $\alpha$  graphite-monochromated radiation,  $\lambda = 0.71073 \text{ \AA}$ ) controlled by the APEX2 software package<sup>[2]</sup> and equipped with an Oxford Cryosystems Series 700 cryostream monitored remotely using the software interface Cryopad.<sup>[3]</sup> X-ray diffraction data for **9** were collected at 180(2)K on a Bruker D8 QUEST equipped with Mo K $\alpha$  sealed tube ( $\lambda = 0.71073 \text{ \AA}$ ), a multilayer TRIUMPH X-ray mirror, a PHOTON 100 CMOS detector, and an Oxford Instruments Cryostrem 700+ Series low temperature device. Diffraction images were processed using the software package SAINT+,<sup>[4]</sup> and data were corrected for absorption by the multiscan semi-empirical method implemented in SADABS.<sup>[5]</sup>

Crystal data for **4e** were instead collected at the Swiss-Norwegian beamline BM01A at the ESRF in Grenoble (France) using synchrotron radiation on the Pilatus@SNBL kappa goniometer from Huber Diffraktionstechnik GmbH, equipped with a Pilatus2M pixel detector from Dectris Ltd. Data collection was performed at low temperature (100 K) using a Cryostream 700 Series from Oxford Cryosystems Ltd. Data integration and empirical absorption corrections were carried out using CrysAlis Pro.<sup>[6]</sup>

All structures were solved using the algorithm implemented in SHELXT-2014,<sup>[7]</sup> which allowed the immediate location of almost all of the heaviest atoms composing the molecular unit of the three compounds. The remaining missing and misplaced non-hydrogen atoms were located from difference Fourier maps calculated from successive full-matrix least-squares refinement cycles on  $F^2$  using the latest SHELXL from the 2014 release.<sup>[8]</sup> All structural refinements were performed using the graphical interface ShelXle.<sup>[9]</sup>

Hydrogen atoms bound to carbon were placed at their idealized positions using appropriate HFIX instructions in SHELXL: 43 (aromatic carbon atoms), 13 (tertiary carbon atoms), 23 ( $-\text{CH}_2-$  carbon atoms) or 137 (for the terminal methyl group). These hydrogen atoms were included in subsequent refinement cycles with isotropic thermal displacement parameters ( $U_{\text{iso}}$ ) fixed at 1.2 (for the three former families of hydrogen atoms) or  $1.5 \times U_{\text{eq}}$  (solely for those associated with the methyl group) of the parent carbon atoms.

In compound **4b**, the terminal methyl group of the pyrandione moiety was found to be disordered over two distinct crystallographic positions, which were modelled into the final crystal structure with fixed rates of occupancy of 33.3 and 66.7%, respectively. Additionally, the crystal structure contains solvent accessible voids which were found to be filled with highly disordered water molecules of crystallisation (a total of 0.25 per molecular unit). Even though it was not possible to locate, or even place geometrically, the hydrogen atoms associated with these solvent molecules, they have been added to the empirical formula.

In compound **4e**, the pyrandione portion composing the spiro moiety was found to be disordered over two distinct crystallographic positions which are approximately rotated by 180° from each other. These two positions were modelled into the final crystal structure with variable, and refineable, rates of occupancy which ultimately converged to values of 80.4(3) and 19.6(3)%, respectively. All non-hydrogen atoms composing these disordered moieties were included in the final structural model with a common refined isotropic displacement parameter.

The last difference Fourier map synthesis showed: for **4b**, the highest peak (0.889 e $\text{\AA}^{-3}$ ) and the deepest hole (-0.354 e $\text{\AA}^{-3}$ ) located at 1.51 and 0.54 Å from O2W and O4,

respectively; for **4e**, the highest peak ( $0.856 \text{ e}\text{\AA}^{-3}$ ) and the deepest hole ( $-0.747 \text{ e}\text{\AA}^{-3}$ ) located at 0.77 and 0.02 Å from O3 and C6, respectively; for **4f**, the highest peak ( $0.769 \text{ e}\text{\AA}^{-3}$ ) and the deepest hole ( $-0.375 \text{ e}\text{\AA}^{-3}$ ) located at 1.06 and 0.38 Å from H7 and C6, respectively. Structural drawings have been created using the software package Crystal Impact Diamond.<sup>[10]</sup>

*Crystal data for **4b**:*  $\text{C}_{23}\text{H}_{20.5}\text{O}_{4.25}$ ,  $M = 364.89$ , trigonal, space group  $R\bar{3}$ ,  $Z = 18$ ,  $a = b = 21.8983(8) \text{ \AA}$ ,  $c = 21.2428(8) \text{ \AA}$ ,  $\alpha = 90^\circ$ ,  $\beta = 90^\circ$ ,  $\gamma = 120^\circ$ ,  $V = 8821.9(7) \text{ \AA}^3$ ,  $\mu(\text{Mo-K}\alpha) = 0.085 \text{ mm}^{-1}$ ,  $D_c = 1.236 \text{ g cm}^{-3}$ , yellow block with crystal size of  $0.17 \times 0.16 \times 0.90 \text{ mm}^3$ . Of a total of 17177 reflections collected, 5224 were independent ( $R_{\text{int}} = 0.0284$ ). Final  $R1 = 0.0603$  [ $|I| > 2\sigma(|I|)$ ] and  $wR2 = 0.2048$  (all data). Data completeness to theta =  $25.24^\circ$ , 99.6%.

*Crystal data for **4e**:*  $\text{C}_{25}\text{H}_{24}\text{O}_6$ ,  $M = 420.44$ , monoclinic, space group  $P2_1/c$ ,  $Z = 4$ ,  $a = 14.1989(3) \text{ \AA}$ ,  $b = 6.32060(10) \text{ \AA}$ ,  $c = 24.2710(5) \text{ \AA}$ ,  $\beta = 96.751(2)^\circ$ ,  $V = 2163.11(7) \text{ \AA}^3$ ,  $\mu(\text{Mo-K}\alpha) = 0.092 \text{ mm}^{-1}$ ,  $D_c = 1.291 \text{ g cm}^{-3}$ , colourless block with crystal size of  $0.04 \times 0.02 \times 0.02 \text{ mm}^3$ . Of a total of 30603 reflections collected, 3923 were independent ( $R_{\text{int}} = 0.0210$ ). Final  $R1 = 0.0632$  [ $|I| > 2\sigma(|I|)$ ] and  $wR2 = 0.1370$  (all data). Data completeness to theta =  $25.40^\circ$ , 99.2%.

*Crystal data for **4f**:*  $\text{C}_{31}\text{H}_{36}\text{O}_4$ ,  $M = 472.60$ , monoclinic, space group  $P2_1/c$ ,  $Z = 4$ ,  $a = 22.418(4) \text{ \AA}$ ,  $b = 9.8837(17) \text{ \AA}$ ,  $c = 11.914(2) \text{ \AA}$ ,  $\beta = 93.040(5)^\circ$ ,  $V = 2636.1(8) \text{ \AA}^3$ ,  $\mu(\text{Mo-K}\alpha) = 0.077 \text{ mm}^{-1}$ ,  $D_c = 1.191 \text{ g cm}^{-3}$ , colourless prism with crystal size of  $0.26 \times 0.26 \times 0.20 \text{ mm}^3$ . Of a total of 56127 reflections collected, 4820 were independent ( $R_{\text{int}} = 0.0397$ ). Final  $R1 = 0.0722$  [ $|I| > 2\sigma(|I|)$ ] and  $wR2 = 0.1963$  (all data). Data completeness to theta =  $25.24^\circ$ , 99.9%.

Crystallographic data (including structure factors) for the crystal structures of compounds **4b**, **4e** and **4f** have been deposited with the Cambridge Crystallographic Data Centre as supplementary publication Nos. CCDC-1527913, -1527914 and -1527915, respectively. Copies of the data can be obtained free of charge on application to CCDC, 12 Union Road, Cambridge CB2 2EZ, U.K. FAX: (+44) 1223 336033. E-mail: [deposit@ccdc.cam.ac.uk](mailto:deposit@ccdc.cam.ac.uk).

## References

- [1] T. Kottke, D. Stalke, *J. Appl. Crystallogr.* **1993**, *26*, 615-619.

- [2] APEX2, *Data Collection Software Version 2.1-RC13*, Bruker AXS, Delft, The Netherlands **2006**.
- [3] Cryopad, *Remote monitoring and control, Version 1.451*, Oxford Cryosystems, Oxford, United Kingdom **2006**.
- [4] SAINT+, *Data Integration Engine v. 8.27b©1997-2012*, Bruker AXS, Madison, Wisconsin, USA.
- [5] G. M. Sheldrick, SADABS 2012/1, *Bruker AXS Area Detector Scaling and Absorption Correction 2012*, Bruker AXS, Madison, Wisconsin, USA.
- [6] CrysAlisPRO, *Oxford Diffraction /Agilent Technologies UK Ltd, Yarnton, England*.
- [7] G. M. Sheldrick, *SHELXT-2014, Program for Crystal Structure Solution, University of Göttingen 2014*.
- [8] (a) G. M. Sheldrick, *Acta Cryst. C* **2015**, 71, 3-8;(b) G. M. Sheldrick, *SHELXL Version 2014, Program for Crystal Structure Refinement, University of Göttingen 2014*;(c) G. M. Sheldrick, *Acta Cryst. A* **2008**, 64, 112-122.
- [9] C. B. Hübschle, G. M. Sheldrick, B. Dittric, *J. Appl. Crystallogr.* **2011**, 44, 1281-1284.
- [10] K. Brandenburg, *DIAMOND, Version 3.2f. Crystal Impact GbR, Bonn, Germany 1997-2010*.